GUFBD / *GUJS* (2022) 12(2): 404-413
DOI: 10.17714/gumusfenbil.1006581 Araştırma Makalesi / *Research Article*

Fabrication of SnS thin film by rapid thermal processing: effect of annealing temperature in sulfurization process

Hızlı ısıl işlemle SnS ince filmlerinin üretimi: sülfürleme işleminde tavlama sıcaklığının etkisi

Ali ÇİRİŞ*[1,a], Mehmet Ali OLGAR[1,2,b]
[1] *Nanotechnology Application and Research Center, Niğde Ömer Halisdemir University, 51240, Niğde*
[2] *Department of Physics, Niğde Ömer Halisdemir University, 51240, Niğde*

• Geliş tarihi / *Received*: 08.10.2021 • Düzeltilerek geliş tarihi / *Received in revised form*: 23.12.2021 • Kabul tarihi / *Accepted*: 16.01.2022

Abstract
In this study, the effect of sulfurization temperature on properties of SnS thin films was investigated. The SnS thin films were fabricated by two-stage method includes deposition of SnS films by magnetron sputtering using a single SnS target, followed by annealing/sulfurization treatment in Rapid Thermal Processing (RTP) system at 225, 300 and 375 °C temperatures. Several characterization techniques such as XRD, Raman spectroscopy, EDX, optical transmission and Van der Pauw were used for analyses of the films. The EDX analyses showed that all the samples had almost stoichiometric (S/Sn~1) chemical composition. However, the amount of sulfur in the samples increased slightly as the sulfurization temperature increased. XRD pattern of the films exhibited constitution of orthorhombic SnS structure regardless of annealing temperature. The SnS_2 secondary phase was observed in addition to orthorhombic SnS phase in the sample annealed at highest reaction temperature (375°C). Raman spectroscopy measurements of the films verified constitution of orthorhombic SnS structure. The band gap of the films exhibited distinction from 1.42 to 1.81 eV regarding to annealing temperature. The electrical characterization of the most promising SnS thin film sulfurized at 300°C had resistivity and charge carrier concentration values 1.07×10^4 Ω.cm and 1.70×10^{14} cm^{-3}, respectively. Based on the all characterizations, it can be deduced that SnS thin film sulfurized at 300°C exhibited more outstanding structural and optical properties for potential solar cell applications.

Keywords: Rapid thermal processing (RTP), RF magnetron sputtering, Sulfurization temperature, Tin sulfide (SnS)

Öz
Bu çalışmada, sülfürleme sıcaklığının SnS ince filmlerin özellikleri üzerine etkisi araştırıldı. SnS ince film örnekleri, RF saçtırma metodunda tek hedef SnS saçtırma kaynağı kullanılarak ile SnS filmlerinin biriktirilmesi ve devamında 225, 300 ve 375°C sıcaklıklarda Hızlı Isıl İşlem (RTP) sistemiyle tavlama/sülfürleme işlemi kullanılmasıyla iki aşamada üretildi. Filmlerin analizleri için XRD, Raman spektroskopisi, EDX, optik geçirgenlik ve Van der Pauw gibi çeşitli karakterizasyon teknikleri kullanıldı. EDX analizleri, tüm numunelerin neredeyse stokiyometrik (S/Sn~1) kimyasal kompozisyona sahip olduğunu gösterdi. Ancak sülfürleme sıcaklığı arttıkça numunelerdeki sülfür miktarının hafifçe arttığı görüldü. Filmlerin XRD spektrumları, tavlama sıcaklığından bağımsız olarak ortorombik SnS yapısının oluşumunu gösterdi. En yüksek sıcaklıkta (375°C) tavlanan SnS örneğinde ortorombik SnS fazının yanında SnS_2 ikincil faz oluşumu gözlendi. Filmlerin Raman spektroskopi ölçümleri, ortorombik SnS yapısının oluşumunu doğruladı. Filmlerin bant aralığının, sülfürleme sıcaklığına bağlı olarak 1.42 ile 1.81 eV arasında değiştiği belirlendi. Sergilediği özellikler ile öne çıkan örnek olan 300°C'de sülfürlenen SnS ince filminin elektriksel karakterizasyonu, özdirenç ve yük taşıyıcı konsantrasyonunun sırasıyla 1.07×10^4 Ω.cm ve 1.70×10^{14} cm^{-3} olduğu belirlendi. Gerçekleştirilen tüm karakterizasyonlara dayanarak, 300°C'de sülfürlenen SnS ince filminin potansiyel güneş hücre uygulamaları için daha üstün yapısal ve optik özelliklere sahip olduğu sonucuna varıldı.

***Anahtar kelimeler**: Hızlı ısıl işlem (RTP), RF mıknatıssal saçtırma, Sülfürleme sıcaklığı, Kalay sülfür (SnS)*

[*a] Ali ÇİRİŞ; aliciris@ohu.edu.tr, Tel: (0388) 225 45 07, orcid.org/0000-0003-4266-2080
[b] orcid.org/0000-0002-6359-8316

1. Introduction
1. Giriş

SnS thin films have been studied as a potential photovoltaic material to overcome some problems encountered in CdTe, Cu(In, Ga)Se_2 (CIGS) etc. thin films that are mostly used in thin film solar cell industry. They suffer from scarcity of In and Ga, toxicity of Cd (Banai et al., 2016; Candelise et al., 2012; Reddy et al., 2010; Tao et al., 2013; Zakutayev, 2017; Zayed & Philippe, 2009). Unlike CdTe and CIGS, SnS has earth-abundant and environmentally friendly raw materials (Fu, 2018; Koteeswara Reddy et al., 2015; Norton et al., 2021). SnS is a binary semiconductor compound that has a direct transition band structure with a band gap between 1.2-1.7 eV (Noguchi et al., 1994; Sorgenfrei et al., 2013), high absorption coefficient (>10^4 cm^{-1}) and p-type conductivity (Vidal et al., 2012; Zhao et al., 2016). All aforementioned properties make this compound very suitable material for photovoltaic applications. Although the SnS semiconductor compound has suitable properties for photovoltaic applications and theoretical limit higher than the 30%, the maximum experimental efficiency is still too low (Shockley & Queisser, 1961; Sinsermsuksakul et al., 2014). The divergence between theoretical and record efficiency value might be accredited to chemical composition, crystalline quality, buffer layer etc. (Di Mare et al., 2017).

The SnS thin films could be prepared by several techniques such as evaporation (Johnson et al., 1999; Noguchi et al., 1994), sputtering (Guang-Pu et al., 1994; Hartman et al., 2011), e-beam evaporation (Gedi et al., 2017; Tanuševski & Poelman, 2003), close space sublimation (Paudel et al., 2015; Zhan et al., 2012), chemical bath deposition (Nair et al., 1991; Ristov et al., 1989), spray pyrolysis (Reddy et al., 2001; Sajeesh et al., 2010), chemical vapor deposition (Kevin et al., 2015; Ortiz et al., 1996), electrodeposition (Ghazali et al., 1998; Zainal et al., 1996). Among these methods, the sputtering method is one of the most preferred method in fabrication of SnS thin films since it provides uniform, high quality, controllable film thickness and mass production ability (Arepalli & Kim, 2018; Arepalli et al., 2019; Son et al., 2020).

It is possible to change morphology, phase-purity, crystallinity and the optical properties of SnS thin films by alteration of deposition parameters such as working pressure, RF power, substrate temperature, etc. (Arepalli & Kim, 2018). Arepalli et al. investigated the effect of working pressure (6 mTorr to 50 mTorr) on properties of SnS thin films. They observed that that the film deposited at 30 mTorr had a more desired grain-growth and surface morphology (Arepalli et al., 2018). Baby et al. showed that the RF power played an active role in the formation secondary phases (such as Sn_2S_3) in SnS thin films. It was seen that the grain structure changed from elongated shape to spherical shape, the sample had non-uniform chemical composition and the band gap shifted by varying the RF power (Baby & Mohan, 2019). In another study, impact of the substrate temperature was investigated. The substrate temperature was increased from room temperature to 420°C. It was seen that large-grained surface morphology obtained by increasing substrate temperature and the best sample prepared by substrate temperature of 350°C (Arepalli & Kim, 2018).

Another important parameter in fabrication of SnS thin film is annealing/sulfurization process which has significant effect on quality of SnS films. This process can be performed by utilizing either Conventional Thermal Processing (CTP) or Rapid Thermal Processing (RTP). The latter one offers much faster heating rate and much shorter annealing time than the CTP system. In this way, the grain growth processes can complete more quickly than the decomposition reactions (Fairbrother et al., 2014).

The SnS thin films can be produced either by deposition of Sn layer followed by sulfurization process or using single source of SnS. The latter strategy is sometimes more proper for fabrication of SnS samples because it offers more homogenous film coating and more facile control of film composition.

Arepalli et al. deposited SnS specimens at room temperature utilizing SnS target by RF sputtering. They investigated effect of deposition pressure on properties of SnS thin films without post-annealing process (Arepalli et al., 2019). Son et al. also followed similar strategy for preparation of SnS samples. They changed the working pressure during the deposition process and obtained the highest efficiency by 0.58% with working pressure of 2.0 Pa. It should be noted that no post-annealing process was applied to deposited films (Son et al., 2020). Rana et al. produced SnS specimens by sputtering employing single source then they annealed the deposited film at 400°C for 1 h in sulfur atmosphere. They found that the sulfurization process improved the crystal structure, resulted in higher carrier concentration,

lower mobility and lower band gap (Rana et al., 2018).
In this study, to the best of our knowledge, this is the first study that examines effect of sulfurization process on properties of SnS samples carried out by RTP method. In this context, SnS samples were fabricated by sputtering method using single SnS target, followed by post-sulfurization process at 225°C, 300°C and 375°C temperatures.

2. Material and method
2. Materyal ve metot

SnS thin film samples were fabricated by RF magnetron sputtering method employing single target of SnS. Before the deposition process, all glass substrates were exposed to cleaning process using acetone, isopropyl alcohol and de-ionized water in ultrasonic cleaner. Then, they were dried utilizing N_2 gas. SnS films were deposited at $3x10^{-3}$ working pressure applying 40 W of RF power. The thickness of films was calibrated to 500 nm. More details on deposition of SnS thin films can be found elsewhere (Olgar et al., 2021).

The sulfurization process was carried out using the RTP furnace. The RTP system carried out the sulfurization process is shown schematically in Figure 1. For the sulfurization process, SnS thin films were placed inside the cylindrical quartz box with a interior volume of 7.6 cm^3. Then, 50 mg of high purity sulfur pieces (99.9995%) were loaded on one side of the quartz box. Finally, the cap of the quartz box was closed to ensure sufficient sulfur pressure inside the box and then was inserted into the RTP vacuum chamber. In order to examine the effect of the post-sulfurization temperature, the treatment was performed at 225°C, 300°C and 375°C temperatures for 5 min in $Ar+H_2$ atmosphere. The ramping rate of heating process was fixed to 3°C/s. After the sulfurization process, the samples were allowed to cool naturally.

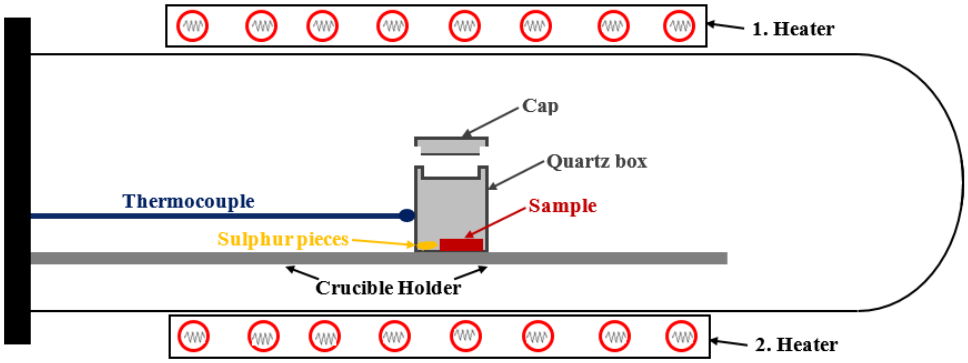

Figure 1. Schematic representation of the RTP furnace employed for the sulfurization process
Şekil 1. *Sülfürleme işlemi için kullanılan RTP fırınının şematik gösterimi*

The samples were labeled according to their sulfurization temperatures, as presented in Table 1. For example, the S-300 sample represents the SnS thin film sulfurized at 300°C. The 'as dep.' is abbreviation of "as-deposited" that is no sulfurization process applied for this sample.

Table 1. Sulfurization temperatures of SnS thin films
Tablo 1. *SnS ince filmlerinin sülfürleme sıcaklıkları*

Sample	Sulfurization Temperature
As dep.	-
S-225	225°C
S-300	300°C
S-375	375°C

X-ray diffraction measurements (XRD) was utilized to investigate structural properties of the prepared samples. Raman spectroscopy measurements have been utilized using 633 nm laser source for verification of SnS phase and distinguishing of secondary phases. The energy dispersive X-ray spectroscopy (EDX) was used for determination of chemical composition of the films. The optical transmission measurements were carried out by spectroscopic ellipsometer (600-1200 nm). Electrical properties of the samples were characterized by Van der Pauw method.

3. Results and discussion
3. Bulgular ve tartışma

The chemical composition of as-deposited (As dep.) and sulfurized SnS samples are shown in Table 2. As shown in Table 2, all of the SnS samples had approximately stoichiometric (S/Sn ~1) chemical composition regardless of the sulfurization process and temperature. Although no remarkable difference was observed in the

chemical composition of the samples, increasing the temperature above the 225°C slightly enhanced sulfur content of the samples (see Table 2). It can be said that sulfurization process at above the 225°C may help diffusion of S atoms in the structure and enhanced the sulfur composition of the films due to sulfurization process.

Table 2. Atomic composition and atomic ratio of SnS thin films
Tablo 2. *SnS ince filmlerinin atomik kompozisyon ve atomik oranı*

Sample	Sn (%)	S (%)	S/Sn
As dep.	50.70	49.30	0.97
S-225	50.80	49.20	0.97
S-300	49.80	50.20	1.01
S-375	49.30	50.70	1.03

The XRD patterns of the as-deposited and sulfurized SnS specimens are displayed in Figure 2. When the XRD pattern of as deposited SnS thin film was examined, it could not be seen a prominent pattern due to amorphous structure of this sample since no annealing process was applied. Contrary to as-deposited sample, when XRD patterns of sulfurized samples were investigated, it was seen that distinct diffraction peaks were observed at around 2θ = 26.5°, 31.6°, 39.1°, 44.7° and 51.0° that correspond to the orthorhombic crystal structure of SnS phase (JCPDS 98-010-6028) (Arepalli og Kim, 2018; Nwofe et al., 2013). It was observed all samples displayed diffraction peaks of orthorhombic crystal structure of SnS irrespective of the sulfurization temperature. In addition to SnS phase, it was observed that the S-375 sample had a weak diffraction peak at around 2θ=15°. This peak may be attributed to the hexagonal SnS_2 phase, Formation of this phase might be due to more sulfur content of this sample (see Table 2). Since SnS thin films can decompose during the sulfurization process, Sn and S atoms may move towards the film surface at different velocity due to differences in the vapor pressure. Due to S inclusion from the sulfurization process, some S atoms may condense on Sn atoms and it causes formation of the SnS_2 phase between the grain boundaries (Naidu et al., 2017). The similar situation was reported in some studies in the literature (Naidu et al., 2017; Patel et al., 2013). Formation of SnS_2 phase in the structure of SnS thin film is undesirable situation since this phase has a detrimental effect on the performance of solar cell that reduces the open circuit voltage (V_{oc}) of the device by forming a diode that behaves as a barrier for charge collection (Wang et al., 2018).

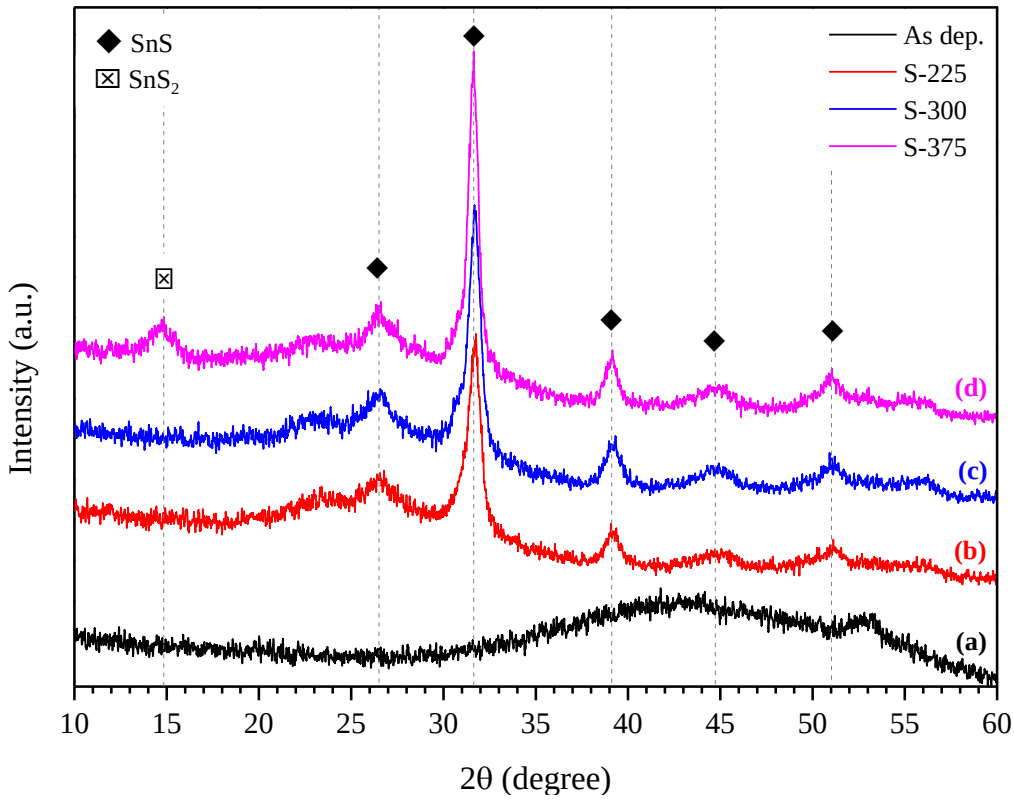

Figure 2. XRD spectra of SnS thin films a) as-deposited and sulfurized at b) 225°C, c) 300°C, d) 375°C
Şekil 2. *a) Sülfürlenmeyen ve b) 225°C c) 300°C d) 375°C'de sülfürlenen SnS ince filmlerinin XRD spektrumları*

In order to examine impact of the sulfurization temperature on structural properties of SnS thin films in more detail, the crystallite size, dislocation density and strains were calculated and presented in Table 3. For this calculation, the full-width at half-maximum (FWHM) values of preferential peak stems from (111) diffraction plane located at around 2θ =31.6° extracted from the XRD patterns (see Figure 2). The crystallite size (D), dislocation density (δ), and strain values (ε) were calculated using the following relations respectively (Chopra, 1969; Patterson, 1939):

$$D = \frac{K\lambda}{\beta\cos\theta} \quad (1)$$

$$\delta = \frac{1}{D^2} \quad (2)$$

$$\varepsilon = \frac{\beta\cos\theta}{4} \quad (3)$$

where K is Scherrer constant (0.94), λ is the wavelength of Cu-K_α irradiation, β is the full width at half maximum (FWHM) and θ is the diffraction angle.

Table 3. Structural parameters of grown SnS samples
Tablo 3. *SnS örneklerinin yapısal parametreleri*

Sample	D (nm)	δ x10^{-3} (nm^{-2})	ε x10^{-3}
As dep.	-	-	-
S-225	11.34	7.77	3.17
S-300	11.81	7.16	3.05
S-375	13.26	5.68	2.71

As displayed in Table 3, when sulfurization temperature increased from 225°C to 375°C the crystallite size enhanced from 11.34 nm to 13.26 nm, the dislocation density decreased from 7.77x10^{-3} nm^{-2} to 5.68x10^{-3} nm^{-2} and strain values decreased from 3.17x10^{-3} to 2.71x10^{-3}. It might be said that arising the sulfurization temperature contributed to enhance the crystallite size and decrease dislocation density and strain in the samples. When taking both XRD patterns and calculated structural parameters into considerations in a body, although the S-375 sample has more promising structural properties, formation of secondary phase (SnS_2) at corresponding annealing temperature indicated that the 300°C temperature is more suitable for SnS sample preparation in terms of secondary phase-free structure. The sulfurization temperature above the 300°C may adversely affect crystal structure of SnS samples in terms of phase purity.

Raman spectra as deposited and sulfurized SnS samples at different temperatures are displayed in Figure 3. A distinct Raman spectrum was not observed for as-deposited SnS thin film as seen in XRD pattern of the same sample. As the sulfurization was applied to as-deposited samples, apparent Raman peaks were observed at 226 cm^{-1} and 289 cm^{-1} that are attributed to the orthorhombic SnS structure (Chandrasekhar et al., 1977). The peak at 226 cm^{-1} corresponds to A_g mode and the 289 cm^{-1} corresponds to the B_{2g} vibration modes of orthorhombic SnS phase (Baby og Mohan, 2018; Chandrasekhar et al., 1977). Irrespective of sulfurization temperature, all samples verified formation of SnS phase, however when the sulfurization temperature increased above to the 300°C, formation of a weak Raman peak at around 312 cm^{-1} was observed. This peak can correspond to the A_{1g} mode of SnS_2 phase (Gurnani et al., 2018; Lee et al., 2017; Smith et al., 1977). These results are consistent with the XRD data of the samples.

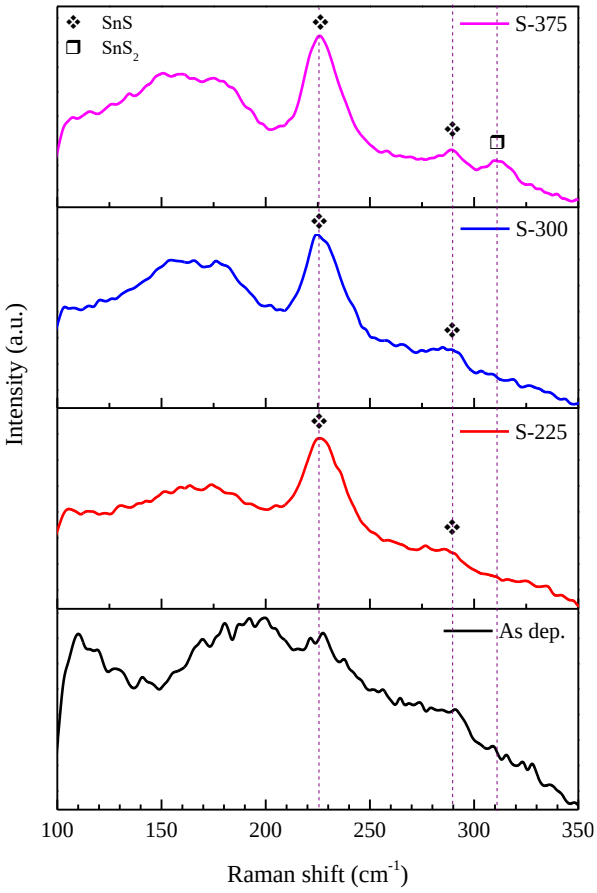

Figure 3. Raman spectra of SnS thin films a) as-deposited and sulfurized at b) 225°C, c) 300°C, d) 375°C
Şekil 3. *a) Sülfürlenmeyen ve b) 225°C c) 300°C d) 375°C'de sülfürlenen SnS ince filmlerinin Raman spektrumları*

Optical properties of SnS samples were investigated by taking optical transmission measurement. The absorption coefficient (α) and optical band gap (E_g) were determined from following formulas respectively (Tauc et al., 1966):

$$\alpha = \frac{1}{d} \mathrm{In}\left(\frac{1}{T}\right) \quad (4)$$

$$(\alpha h\nu) = A\left(h\nu - E_g\right)^{1/2} \quad (5)$$

where d represents thickness of the film, T is transmittance, A is constant and hν is the energy of the photon. The optical band gaps were determined by taking interception on the horizontal axis of $(\alpha h\nu)^2$-(hν) curve (see Figure 4). In this regard, the calculated band gap values are listed in Table 4. It was seen that the as deposited sample had 1.81 eV band gap value and the sulfurized samples had values varied from 1.42 eV to 1.71 eV due to sulfurization process and temperature. The obtained band gap values are consistent with literature (Ceylan, 2017; Hasan og Shallal, 2014; Jain og Arun, 2013; Javed et al., 2020; Sousa et al., 2014). It was determined that as the uprising the sulfurization temperature up to 300°C, the band gap decreased up to 1.42 eV that is nearly optimal band gap for SnS phase reported in the literature. However, the band gap of the films increased from 1.42 eV to 1.67 eV by increasing the sulfurization temperature from 300°C to 375°C that is higher than the optimal band gap value. The distinction in optical band gaps may be ascribed to crystalline quality, stoichiometric deviations and grain structure (Guo et al., 2017; Jain og Arun, 2013).

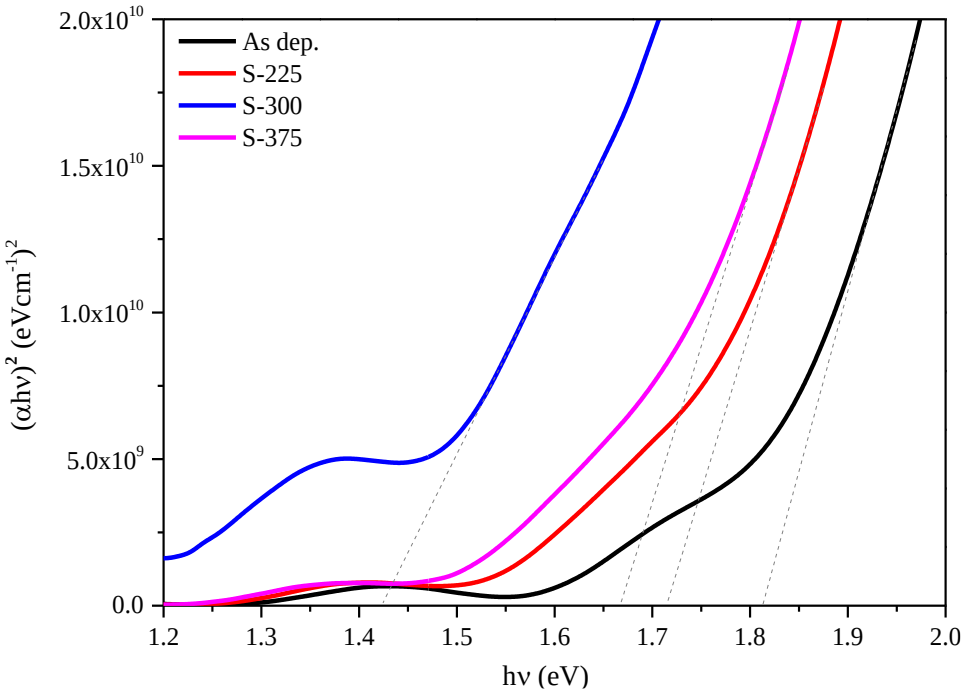

Figure 4. Plots of $(\alpha h\nu)^2$ - (hν) of SnS thin films for estimation of optical band gaps
Şekil 4. *Optik bant aralıklarının belirlenmesi için SnS ince fimlerinin $(\alpha h\nu)^2$ - (hν) grafikleri*

Table 4. The band gap values of as deposited and sulfurized SnS thin films
Tablo 4. *Sülfürlenmeyen ve sülfürlenen Sn Since filmlerinin yasak enerji değerleri*

Sample	E_g (eV)
As dep.	1.81
S-225	1.71
S-300	1.42
S-375	1.67

Electrical characterization of the samples demonstrated that all samples showed p-type conductivity regardless of the sulfurization temperature. The electrical properties (resistivity and carrier concentration) of SnS samples are summarized in Table 5. As summarized in the Table 5, it was found that the resistivity of the samples were about 10^4 Ω.cm and carrier concentration values were about 10^{14} cm^{-3} that are compatible with the reported studies in the literature (Chalapathi et al., 2020; Park et al., 2015). When taking electrical properties of the samples into consideration, it was observed that the sulfurization process and temperature has no remarkable impact on electrical properties of the films.

Table 5. Electrical properties of as-deposited and sulfurized SnS thin films
Tablo 5. *Sülfürlenmeyen ve sülfürlenen SnS ince filmlerinin elektriksel özellikleri*

Sample	Resistivity (Ω.cm)	Carrier concentration (cm^{-3})
As dep.	1.35 x10^4	1.70 x10^{14}
S-225	1.32 x10^4	2.22 x10^{14}
S-300	1.07 x10^4	1.70 x10^{14}
S-375	1.12 x10^4	1.12 x10^{14}

4. Conclusion
4. Sonuçlar

In this study, the effect of sulfurization temperature on structural, optical and electrical properties of SnS thin films was investigated. The SnS samples were prepared by two-stage process includes sputter deposition of SnS thin film using single target followed by the sulfurization process carried out at 225, 300 and 375°C temperatures employing RTP method. The EDX results showed that all samples had nearly stoichiometric (S/Sn~1) composition, however higher annealing temperature (> 300°C) gave rise to excess of sulfur content in the structure. The XRD patterns showed that orthorhombic SnS phase formed in all samples regardless of the sulfurization temperature. However, the SnS_2 secondary phase also formed in S-375 sample in addition to SnS phase. In addition, increasing the sulfurization temperature enhanced crystallite size, reduced the dislocation density and decreased strain in the lattice of the samples. The Raman spectra confirmed formation of SnS phase in all samples and SnS_2 phase only in S-375 sample that is consistent with XRD data of the samples. Optical band gap values decreased from 1.81 eV to 1.42 eV with sulfurization process. Electrical characterizations showed that all samples had resistivity values about 10^4 Ω.cm and carrier concentration values about 10^{14} cm^{-3}. Considering the all characterization results, it can be concluded that higher sulfurization temperatures (≥300°C) yielded more proper structural, optical and electrical properties in SnS thin films. The sulfurization of SnS thin films at 300°C presented more promising properties amongst other samples for potential photovoltaic application.

Acknowledgements
Teşekkür

The authors wish to acknowledge Dr. Murat Tomakin for optical and electrical measurements.

Author contribution
Yazar Katkısı

Ali ÇİRİŞ: Conceptualization, Methodology, Writing - original draft, Writing - review & editing. Mehmet Ali OLGAR: Conceptualization, Methodology, Writing - original draft, Writing - review & editing.

Declaration of ethical code
Etik beyanı

The article authors declare that the materials and methods used in this study do not require ethical committee approval and/or legal-specific permission.

Conflicts of interest
Çıkar çatışması beyanı

The authors declare that they have no known competing financial interests or personal relationships that could have appeared to influence the work reported in this paper.

References
Kaynaklar

Arepalli, V. K., & Kim, J. (2018). Effect of substrate temperature on the structural and optical properties of radio frequency sputtered tin sulfide thin films for solar cell application. *Thin Solid Films*, *666*, 34-39. https://doi.org/10.1016/j.tsf.2018.09.009

Arepalli, V. K., Shin, Y., & Kim, J. (2018). Influence of working pressure on the structural, optical, and electrical properties of rf-sputtered sns thin films. *Superlattices and Microstructures*, *122*, 253-261. https://doi.org/10.1016/j.spmi.2018.08.001

Arepalli, V. K., Shin, Y., & Kim, J. (2019). Photovoltaic behavior of the room temperature grown rf-sputtered sns thin films. *Optical Materials*, *88*, 594-600. v10.1016/j.optmat.2018.12.016

Baby, B. H., & Mohan, D. B. (2018). Phase optimization study of orthorhombic structured sns nanorods from ctab assisted polyol synthesis for higher efficiency thin film solar cells. *Solar Energy*, *174*, 373-385. https://doi.org/10.1016/j.solener.2018.09.019

Baby, B. H., & Mohan, D. B. (2019). The effect of in-situ and post deposition annealing towards the structural optimization studies of rf sputtered sns and sn2s3 thin films for solar cell application. *Solar Energy*, *189*, 207-218. https://doi.org/10.1016/j.solener.2019.07.059

Banai, R. E., Horn, M. W., & Brownson, J. R. S. (2016). A review of tin (ii) monosulfide and its potential as a photovoltaic absorber. *Solar energy materials and solar cells, 150*, 112-129. https://doi.org/10.1016/j.solmat.2015.12.001

Candelise, C., Winskel, M., & Gross, R. (2012). Implications for cdte and cigs technologies production costs of indium and tellurium scarcity. *Progress in Photovoltaics, 20*(6), 816-831. https://doi.org/10.1002/pip.2216

Ceylan, A. (2017). Synthesis of sns thin films via high vacuum sulfidation of sputtered sn thin films. *Materials Letters, 201*, 194-197. https://doi.org/10.1016/j.matlet.2017.05.022

Chalapathi, U., Poornaprakash, B., Choi, W. J., & Park, S. H. (2020). Ammonia(aq)-enhanced growth of cubic sns thin films by chemical bath deposition for solar cell applications. *Applied Physics a-Materials Science & Processing, 126*(8), 1-9. https://doi.org/10.1007/s00339-020-03763-4

Chandrasekhar, H., Humphreys, R., Zwick, U., & Cardona, M. (1977). Infrared and raman spectra of the iv-vi compounds sns and snse. *Physical Review B, 15*(4), 2177. https://doi.org/10.1103/PhysRevB.15.2177

Chopra, K. (1969). Thin film phenomena mcgraw-hill. *New York, 19692*, 196.

Di Mare, S., Menossi, D., Salavei, A., Artegiani, E., Piccinelli, F., Kumar, A., Mariotto, G., & Romeo, A. (2017). Sns thin film solar cells: Perspectives and limitations. *Coatings, 7*(2), 34. https://doi.org/10.3390/coatings7020034

Fairbrother, A., Fourdrinier, L., Fontané, X., Izquierdo-Roca, V., Dimitrievska, M., Pérez-Rodríguez, A. ,& Saucedo, E. (2014). *Rapid thermal processing of $cu_2znsnse_4$ thin films.* Í *2014 IEEE 40th Photovoltaic Specialist Conference (PVSC)*. https://doi.org/10.1109/PVSC.2014.6925390

Fu, H. Y. (2018). Environmentally friendly and earth-abundant colloidal chalcogenide nanocrystals for photovoltaic applications. *Journal of Materials Chemistry C, 6*(3), 414-445. https://doi.org/10.1039/c7tc04952h

Gedi, S., Reddy, V. R. M., Kang, J. Y., & Jeon, C. W. (2017). Impact of high temperature and short period annealing on sns films deposited by e-beam evaporation. *Applied Surface Science, 402*, 463-468. https://doi.org/10.1016/j.apsusc.2017.01.113

Ghazali, A., Zainal, Z., Hussein, M. Z., & Kassim, A. (1998). Cathodic electrodeposition of sns in the presence of edta in aqueous media. *Solar energy materials and solar cells, 55*(3), 237-249. https://doi.org/10.1016/S0927-0248(98)00106-8

Guang-Pu, W., Zhi-Lin, Z., Wei-Ming, Z., Xiang-Hong, G., Wei-Qun, C., Tanamura, H., Yamaguchi, M., Noguchi, H., Nagatomo, T., & Omoto, O. (1994). *Investigation on sns film by rf sputtering for photovoltaic application.* Í *Proceedings of 1994 IEEE 1st World Conference on Photovoltaic Energy Conversion-WCPEC (A Joint Conference of PVSC, PVSEC and PSEC)*. https://doi.org/10.1109/WCPEC.1994.519977

Guo, F. R., Guo, H. F., Zhang, K. Z., Yuan, N. Y., & Ding, J. N. (2017). Variations in structural and optoelectronic features of thermally co-evaporated sns films with different sn contents. *Thin Solid Films, 642*, 285-289. https://doi.org/10.1016/j.tsf.2017.09.031

Gurnani, C., Hawken, S. L., Hector, A. L., Huang, R., Jura, M., Levason, W., Perkins, J., Reid, G., & Stenning, G. B. (2018). Tin(iv) chalcogenoether complexes as single source precursors for the chemical vapour deposition of sne_2 and sne (e= s, se) thin films. *Dalton Transactions, 47*(8), 2628-2637. https://doi.org/10.1039/C7DT03848H

Hartman, K., Johnson, J. L., Bertoni, M. I., Recht, D., Aziz, M. J., Scarpulla, M. A., & Buonassisi, T. (2011). Sns thin-films by rf sputtering at room temperature. *Thin Solid Films, 519*(21), 7421-7424. https://doi.org/10.1016/j.tsf.2010.12.186

Hasan, B. A., & Shallal, I. H. (2014). Structural and optical properties of sns thin films. *Journal of Nanotechnology & Advance Materials*(2), 43-49. https://doi.org/10.18576/jnam

Jain, P., & Arun, P. (2013). Influence of grain size on the band-gap of annealed sns thin films. *Thin Solid Films, 548*, 241-246. https://doi.org/10.1016/j.tsf.2013.09.089

Javed, A., Khan, N., Bashir, S., Ahmad, M., & Bashir, M. (2020). Thickness dependent structural, electrical and optical properties of cubic sns thin films. *Materials Chemistry and Physics, 246*, 122831. https://doi.org/10.1016/j.matchemphys.2020.122831

Johnson, J. B., Jones, H., Latham, B. S., Parker, J. D., Engelken, R. D., & Barber, C. (1999). Optimization of photoconductivity in vacuum-evaporated tin sulfide thin films. *Semiconductor Science and Technology, 14*(6), 501-507. https://doi.org/10.1088/0268-1242/14/6/303

Kevin, P., Lewis, D. J., Raftery, J., Malik, M. A., & O'Brien, P. (2015). Thin films of tin(ii) sulphide (sns) by aerosol-assisted chemical vapour deposition (aacvd) using tin(ii) dithiocarbamates as single-source precursors. *Journal of Crystal Growth, 415*, 93-99. https://doi.org/10.1016/j.jcrysgro.2014.07.019

Koteeswara Reddy, N., Devika, M., & Gopal, E. (2015). Review on tin (ii) sulfide (sns) material: Synthesis, properties, and applications. *Critical Reviews in Solid State and Materials Sciences, 40*(6), 359-398. https://doi.org/10.1080/10408436.2015.1053601

Lee, S., Shin, S., Ham, G., Lee, J., Choi, H., Park, H., & Jeon, H. (2017). Characteristics of layered tin disulfide deposited by atomic layer deposition with h_2s annealing. *AIP Advances, 7*(4), 045307. https://doi.org/10.1063/1.4982068

Naidu, R., Loorits, M., Karber, E., Volobujeva, O., Raudoja, J., Maticiuc, N., Bereznev, S., & Mellikov, E. (2017). Impact of vacuum and nitrogen annealing on hve sns photoabsorber films. *Materials Science in Semiconductor Processing, 71*, 252-257. https://doi.org/10.1016/j.mssp.2017.08.004

Nair, M. T. S., Nair, P. K., & Nair, P. K. (1991). Simplified chemical-deposition technique for good quality sns thin-films. *Semiconductor Science and Technology, 6*(2), 132-134. https://doi.org/10.1088/0268-1242/6/2/014

Noguchi, H., Setiyadi, A., Tanamura, H., Nagatomo, T., & Omoto, O. (1994). Characterization of vacuum-evaporated tin sulfide film for solar-cell materials. *Solar energy materials and solar cells, 35*(1-4), 325-331. https://doi.org/10.1016/0927-0248(94)90158-9

Norton, K. J., Alam, F., & Lewis, D. J. (2021). A review of the synthesis, properties, and applications of bulk and two-dimensional tin (ii) sulfide (sns). *Applied Sciences-Basel, 11*(5), 2062. https://doi.org/10.3390/app11052062

Nwofe, P. A., Miles, R. W., & Reddy, K. T. R. (2013). Effects of sulphur and air annealing on the properties of thermally evaporated sns layers for application in thin film solar cell devices. *Journal of Renewable and Sustainable Energy, 5*(1), 011204. https://doi.org/10.1063/1.4791784

Olgar, M. A., Ciri, A., Tomakin, M., & Zan, R. (2021). Impact of in/ex situ annealing and reaction temperature on structural, optical and electrical properties of sns thin films. *Journal of Molecular Structure, 1241*, 130631. https://doi.org/10.1016/j.molstruc.2021.130631

Ortiz, A., Alonso, J. C., Garcia, M., & Toriz, J. (1996). Tin sulphide films deposited by plasma-enhanced chemical vapour deposition. *Semiconductor Science and Technology, 11*(2), 243-247. https://doi.org/10.1088/0268-1242/11/2/017

Park, H. H., Heasley, R., Sun, L. Z., Steinmann, V., Jaramillo, R., Hartman, K., Chakraborty, R., Sinsermsuksakul, P., Chua, D., Buonassisi, T., & Gordon, R. G. (2015). Co-optimization of sns absorber and zn(o,s) buffer materials for improved solar cells. *Progress in Photovoltaics, 23*(7), 901-908. v10.1002/pip.2504

Patel, M., Mukhopadhyay, I., & Ray, A. (2013). Annealing influence over structural and optical properties of sprayed sns thin films. *Optical Materials, 35*(9), 1693-1699. https://doi.org/10.1016/j.optmat.2013.04.034

Patterson, A. (1939). The scherrer formula for x-ray particle size determination. *Physical review, 56*(10), 978. https://doi.org/10.1103/PhysRev.56.978

Paudel, N. R., Xiao, C., & Yan, Y. (2015). *Study of close space sublimation (css) grown sns thin-films for solar cell applications.* Í *2015 IEEE 42nd Photovoltaic Specialist Conference (PVSC)*. https://doi.org/10.1109/PVSC.2015.7356115

Rana, T. R., Kim, S., & Kim, J. (2018). Existence of multiple phases and defect states of sns absorber and its detrimental effect on efficiency of sns solar cell. *Current Applied Physics, 18*(6), 663-666. https://doi.org/10.1016/j.cap.2018.03.024

Reddy, K. T. R., Prathap, P., & Miles, R. W. (2010). Thin films of tin sulphide for application in photovoltaic solar cells. *Photovoltaics: developments, applications and impact*, 37-61.

Reddy, K. T. R., Reddy, P. P., Miles, R. W., & Datta, P. K. (2001). Investigations on sns films deposited by spray pyrolysis. *Optical Materials, 17*(1-2), 295-298. https://doi.org/10.1016/S0925-3467(01)00052-0

Ristov, M., Sinadinovski, G., Grozdanov, I., & Mitreski, M. (1989). Chemical deposition of tin (ii) sulphide thin films. *Thin Solid Films, 173*(1), 53-58. https://doi.org/10.1016/0040-6090(89)90536-1

Sajeesh, T. H., Warrier, A. R., Kartha, C. S., & Vijayakumar, K. P. (2010). Optimization of parameters of chemical spray pyrolysis technique to get n and p-type layers of sns. *Thin Solid Films, 518*(15), 4370-4374. https://doi.org/10.1016/j.tsf.2010.01.040

Shockley, W., & Queisser, H. J. (1961). Detailed balance limit of efficiency of p-n junction solar cells. *Journal of Applied Physics, 32*(3), 510-519. https://doi.org/10.1063/1.1736034

Sinsermsuksakul, P., Sun, L. Z., Lee, S. W., Park, H. H., Kim, S. B., Yang, C. X., & Gordon, R. G. (2014). Overcoming efficiency limitations of sns-based solar cells. *Advanced Energy Materials, 4*(15), 1400496. https://doi.org/10.1002/aenm.201400496

Smith, A., Meek, P., & Liang, W. (1977). Raman scattering studies of sns_2 and $snse_2$. *Journal of Physics C: Solid State Physics*, *10*(8), 1321. https://doi.org/10.1088/0022-3719/10/8/035

Son, S. I., Shin, D., Son, Y. G., Son, C. S., Kim, D. R., Park, J. H., Kim, S., Hwang, D., & Song, P. (2020). Effect of working pressure on the properties of rf sputtered sns thin films and photovoltaic performance of sns-based solar cells. *Journal of Alloys and Compounds*, *831*, 154626. https://doi.org/10.1016/j.jallcom.2020.154626

Sorgenfrei, T., Hofherr, F., Jauss, T., & Croll, A. (2013). Synthesis and single crystal growth of sns by the bridgman-stockbarger technique. *Crystal Research and Technology*, *48*(4), 193-199. https://doi.org/10.1002/crat.201200484

Sousa, M. G., da Cunha, A. F., & Fernandes, P. A. (2014). Annealing of rf-magnetron sputtered sns2 precursors as a new route for single phase sns thin films. *Journal of Alloys and Compounds*, *592*, 80-85. https://doi.org/10.1016/j.jallcom.2013.12.200

Tanuševski, A., & Poelman, D. (2003). Optical and photoconductive properties of sns thin films prepared by electron beam evaporation. *Solar energy materials and solar cells*, *80*(3), 297-303. https://doi.org/10.1016/j.solmat.2003.06.002

Tao, C. S., Jiang, J., & Tao, M. (2013). *Natural resource limitations to terawatt-scale solar photovoltaics.* Í *2013 Twentieth International Workshop on Active-Matrix Flatpanel Displays and Devices (AM-FPD)*.

Tauc, J., Grigorovici, R., & Vancu, A. (1966). Optical properties and electronic structure of amorphous germanium. *physica status solidi (b)*, *15*(2), 627-637. https://doi.org/10.1002/pssb.19660150224

Vidal, J., Lany, S., d'Avezac, M., Zunger, A., Zakutayev, A., Francis, J., & Tate, J. (2012). Band-structure, optical properties, and defect physics of the photovoltaic semiconductor sns. *Applied physics letters*, *100*(3), 032104. https://doi.org/10.1063/1.3675880

Wang, W., Chen, G., Cai, H., Chen, B., Yao, L., Yang, M., Chen, S., & Huang, Z. (2018). The effects of sns_2 secondary phases on cu_2znsns_4 solar cells: A promising mechanical exfoliation method for its removal. *Journal of Materials Chemistry A*, *6*(7), 2995-3004. https://doi.org/10.1039/C7TA08242H

Zainal, Z., Hussein, M. Z., & Ghazali, A. (1996). Cathodic electrodeposition of sns thin films from aqueous solution. *Solar energy materials and solar cells*, *40*(4), 347-357. https://doi.org/10.1016/0927-0248(95)00157-3

Zakutayev, A. (2017). Brief review of emerging photovoltaic absorbers. *Current Opinion in Green and Sustainable Chemistry*, *4*, 8-15. https://doi.org/10.1016/j.cogsc.2017.01.002

Zayed, J., & Philippe, S. (2009). Acute oral and inhalation toxicities in rats with cadmium telluride. *Int J Toxicol*, *28*(4), 259-265. https://doi.org/10.1177/1091581809337630

Zhan, X. P., Shi, C. W., Shen, X. J., Yao, M., & Zhang, Y. R. (2012). *Preparation of sns thin films by close-spaced sublimation at different source temperatures.* Í *Advanced Materials Research*. https://doi.org/10.4028/www.scientific.net/AMR.590.148

Zhao, L. B., Di, Y. X., Yan, C., Liu, F. Y., Cheng, Z., Jiang, L. X., Hao, X. J., Lai, Y. Q., & Li, J. (2016). In situ growth of sns absorbing layer by reactive sputtering for thin film solar cells. *RSC advances*, *6*(5), 4108-4115. https://doi.org/10.1039/c5ra24144h